

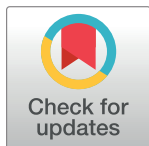
RESEARCH ARTICLE

Hydrothermal assisted biogenic synthesis of silver nanoparticles: A potential study on virulent candida isolates from COVID-19 patients

Fatma O. Khalil¹, Muhammad B. Taj^{2*}, Enas M. Ghonaim¹, Shimaa Abed El-Sattar³, Sally W. Elkhadry⁴, Hala El-Refai¹, Omar M. Ali^{5*}, Ahmed Salah A. Elgawad⁶, Heba Alshater⁷

1 Clinical and Molecular Microbiology and Immunology Department, National Liver Institute, Menoufia University, Shebin El-Kom, Egypt, **2** Division of Inorganic Chemistry, Institute of Chemistry, The Islamia University Bahawalpur, Bahawalpur, Pakistan, **3** Clinical Biochemistry and Molecular Diagnostics, National Liver Institute, Menoufia University, Shebin El-Kom, Egypt, **4** Epidemiology and Preventive Medicine Department, National Liver Institute, Menoufia University, Shebin El-Kom, Egypt, **5** Department of Chemistry, Turabah University College, Turabah Branch, Taif University, Taif Saudi Arabia, **6** Department of Clinical Pathology, National Liver Institute, Menoufia University Hospital, Menoufia University, Shebin El-Kom, Egypt, **7** Department of Forensic Medicine and Clinical Toxicology, Menoufia University Hospital, Menoufia University, Shebin El-Kom, Egypt

* dr.taj@iub.edu.pk (MBT); om.ali@tu.edu.sa (OMA)



OPEN ACCESS

Citation: Khalil FO, Taj MB, Ghonaim EM, Abed El-Sattar S, Elkhadry SW, El-Refai H, et al. (2022) Hydrothermal assisted biogenic synthesis of silver nanoparticles: A potential study on virulent candida isolates from COVID-19 patients. PLoS ONE 17(10): e0269864. <https://doi.org/10.1371/journal.pone.0269864>

Editor: Amitava Mukherjee, VIT University, INDIA

Received: January 5, 2022

Accepted: May 27, 2022

Published: October 6, 2022

Copyright: © 2022 Khalil et al. This is an open access article distributed under the terms of the [Creative Commons Attribution License](https://creativecommons.org/licenses/by/4.0/), which permits unrestricted use, distribution, and reproduction in any medium, provided the original author and source are credited.

Data Availability Statement: All relevant data are within the paper.

Funding: There is no amendment in the funding statement (Omar M. Ali This study has been funded by the Taif University Researchers Supporting Project number (TURSP-2020/81).

Competing interests: The authors have declared that no competing interests exist.

Abstract

Till now the exact mechanism and effect of biogenic [silver nanoparticles](#) on fungus is an indefinable question. To focus on this issue, the first time we prepared hydrothermal assisted thyme coated silver nanoparticles (T/AgNPs) and their toxic effect on *Candida* isolates were determined. The role of *thyme* (*Thymus Vulgaris*) in the reduction of silver ions and stabilization of T/AgNPs was estimated by Fourier transforms infrared spectroscopy, structure and size of present silver nanoparticles were detected via atomic force microscopy as well as high-resolution transmission electron microscopy. The biological activity of T/AgNPs was observed against *Candida* isolates from COVID-19 Patients. Testing of virulence of *Candida* species using Multiplex PCR. T/AgNPs proved highly effective against *Candida albicans*, *Candida kruzei*, *Candida glabrata* and MIC values ranging from 156.25 to 1,250 µg/mL and MFC values ranging from 312.5 to 5,000 µg/mL. The structural and morphological modifications due to T/AgNPs on *Candida albicans* were detected by TEM. It was highly observed that when *Candida albicans* cells were subjected to 50 and 100 µg/mL T/AgNPs, a remarkable change in the cell wall and cell membrane was observed.

Introduction

The severe acute respiratory syndrome coronavirus 2 (SARS-CoV-2) is the primary infectious agent of Coronavirus Disease 2019 (COVID-19), a rapidly spreading pneumonia [1]. It is confronting the global public health system. SARS-CoV-2 infects any age with a high impact on

the elder people other than SARS-CoV and MERS-CoV [2]. Aside from the pathogenicity of SARS-CoV-2, microbial infections play a crucial role in the occurrence as well as the progression of SARS-CoV-2 infection by making a diagnosis, prognosis, and treatment of COVID-19 more difficult, as well as increasing illness symptoms and mortality [3]. *Candida* strains have been reported in the skin and mucosal dwellers that cause a variety of devastating diseases in immunosuppressed individuals and those who are susceptible [4]. *Candida* species possess numerous virulence factors, including exoenzymes like phospholipase as well as protease, or the capacity to generate the germ tubes and cling to buccal epithelial cells, that aid in the adherence as well as the intrusion of these organisms through the cell membrane, malfunctioning or rupturing [5]. The improper handling of antimicrobial drugs may enhance the prevalence of drug-resistant pathogens [6]. A major cause for the failure of antifungal treatment is low penetration potential to the infection site as well as their side effects [7].

Nanotechnology is one of the promising areas of science that has shown its impact on all scientific fields equally [8, 9]. Nanosized materials, having a size of 20–100 nm, have attracted the attention of researchers because of their propitious characteristics [10]. Engineered silver nanoparticles (AgNPs) have shown their outstanding applications in food-related fields owing to their remarkable antifungal activities [11, 12] and are widely applicable in the biomedical field like cancer photodynamic therapy, biomedical sensing, and molecular imaging as well as drug delivery [13]. Synthesis of nanoparticles via green strategy such as by using plant extract [14], enzymes, phytochemicals etc are preferred mostly as compared to chemically manufactured nanosized material owing to overcome its toxic effect on the environment and living beings [15].

Thymus vulgaris L. plant has tremendous medical applications as it was used previously to treat various diseases like stiffening of arteries, urinary tract infections, dyspepsia, pneumonia, respiratory disorders (asthma, bronchitis, or cough), toothache, endocarditis [16–18] and septicemia due to the presence of biochemical in it and it gains the status of the General Recognized as Safe (GRAS) defined by Food and Drug Administration (FDA) [19]. Thymol in *Thymus vulgaris L.* can destroy the cell membrane of microorganisms [20–22].

In most antifungal treatments, the main biological resistance to drug diffusion is the formation of biofilm that is formed by the aggregation of *Candida albicans* [23, 24]. Drug diffusion decreases due to the formation of biofilm that enhances the cell viscosity [25, 26]. The exact mechanism for antifungal treatment is still unknown for thyme coated silver nanoparticles. The present study aims to develop a low cost sustainable hydrothermal method without the addition of any base and with minimum involvement of energy to explore the application and effect of T/AgNPs on membrane damage against *Candida* isolates from Covid-19 patients. Up to our knowledge use of *Thymus vulgaris* extract in the hydrothermal approach has not been reported yet.

Materials and methods

This is a cross-sectional study done using fungal isolates from COVID-19 patients admitted patients of Menoufia Faculty of Medicine, Menoufia University Hospital after patient's consent (verbal) and approval of Research Ethics Committee of faculty of medicine, Menoufia University (IRB No. 312021/FORE8). Fungal identification Antifungal testing and molecular detection of virulence factors were done in the Microbiological Laboratory, National liver Institute, Menoufia University. All chemicals as well as solvents were of analytical grade and were not purified further.

Plant material

The *Thymus vulgaris* plant was collected from Egypt. The plant was distinguished at the office of Botany, Faculty of Science, Menoufia University, Shebin El-Kom, Egypt where voucher examples were stored. *Thymus vulgaris* plant was were rinsed with distilled water, weighted, and frozen (-20°C). After lyophilization (Dura Dry TM μP freeze-drier; -45°C and 250 mTorr), it was properly stored till used for extraction and synthesis [27].

Preparation of plant extract

Fresh plant leaves were steeped in 70 percent ethanol/water (100 ml) at room temperature for 7 days after being cleaned with tap water and finally with deionized water. It was then filtered by utilizing Whatman filter paper no. 1 The extract was then warmed to 4°C and stored for future use [28].

Synthesis of silver nanoparticles

Thyme covered silver nanoparticles were synthesized by the modified hydrothermal method [29]. A 25 ml of 0.25 M silver nitrate solution was mixed with 25 ml of plant extract and stirred at 35°C for 1 h. This solution mixture was transferred into Teflon lined sealed stainless-steel autoclaves and kept in a hydrothermal oven at a temperature of 150°C for 1.5 h. Then the contents are allowed to cool to room temperature. Pure dark brown colored T/AgNPs were collected by centrifugation at 5000 rpm for 10 minutes. The stable T/AgNPs were dried in an oven at 60°C for 4 h, ground, and preserved in an airtight bottle (Fig 1).

Characterization of silver nanoparticles

The analysis was carried out at National Research Centre in Cairo Egypt. A Jasco dual-beam spectrophotometer was used to record the UV-vis spectroscopy estimates (model UV-VIS-NIR 570) operated at a resolution of 2 nm. FTIR measurements were recorded on Perkin Elmer Inc ranging from 4000 nm to 650 nm. Morphological ponders were employed utilizing high-resolution transmission electron microscopy (HRTEM). The HRTEM images were gotten by a JEOL-JEM-2100 version and an atomic force microscope (AFM) was used to determine surface topography and roughness profiles of Nanomaterials using Model 5600LS manufactured by Agilent technology company in the USA. The biological study was implemented in the National Liver Institute, Menoufia University during the period from May 2020 to February 2021 on different samples isolated from COVID-19 patients. The samples were inoculated on Sabrouds dextrose agar (HiMedia, India) and colonies identified by Gram staining, morphology on cornmeal agar, germ tube tests, and chromogenic medium (HiMedia,

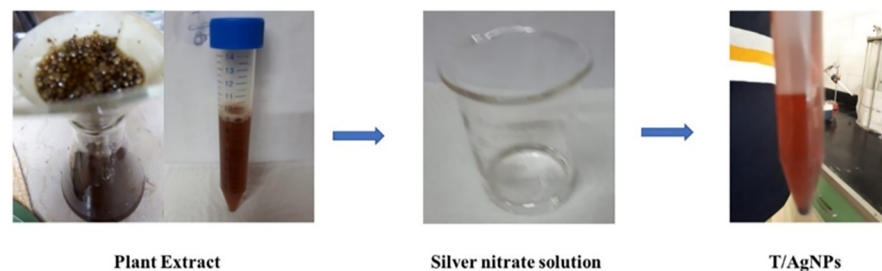


Fig 1. Synthesis of T/AgNPs by plant extract.

<https://doi.org/10.1371/journal.pone.0269864.g001>

Mumbai, India), and further identification and antifungal sensitivity were done by the VITEK-2 Yeast identification and AST card (BioMérieux).

Biological activities

DNA extraction. The QIAamp DNA Mini kit (Qiagen, Germany, GmbH) was used to isolate DNA from samples, with certain changes based on the manufacturer's instructions. A 200 µl sample suspension was incubated at 56 °C for 10 minutes with 10µl proteinase K and 200 µl lysis buffer. Following that, 200 microliters of 100 percent ethanol were poured over the lysate. After that, a centrifuge was used to separate the solution. The nucleic acid was extracted with 100 µl of the kit's elution buffer.

PCR amplification. *Oligonucleotide primer.* The primers used were provided by Metabion (Germany) and are listed in (Table 1). A 25 µl reaction including 12.5 µl of EmeraldAmp Max PCR Master Mix (Takara, Japan), 1 µl of each primer at 20 pmol concentration, 5.5 µl of water, and 5 µl of DNA template was used to test the primers. An Applied biosystems 2720 thermal cycler was used to carry out the reaction.

Analysis of the PCR products. The PCR products were eluted out using 5V/cm gradients on a 1.5 percent agarose gel (Applichem, Germany, GmbH) in 1x TBE buffer at room temperature. 15 µl of the products were inserted into each gel slot for analysis. The fragment sizes were determined using a general 100 bp ladder (Fermentas, Germany) as well as gelpilot 100 bp ladders. A gel documentation system (Alpha Innotech, Biometra) was used to photograph the gel, and the data was processed using computer software. (Table 3) lists the target genes, primer sequences cycle conditions and amplicon sizes [28].

Antifungal susceptibility testing. The antifungal effect of biosynthetic T/AgNPs was evaluated on virulent *Candida albicans* and *non-albicans* isolates using the disc diffusion method using discs; Nystatin 100 U, Clotrimazole 10µg, Fluconazole 10µL, Voriconazole 10µg, Itraconazole 10µg, the results obtained were compared for T/AgNPs formed by using the chemical strategy and *Thymus vulgaris*. The disk diffusion method shows the magnitude of the susceptibility of the virulent fungi. The Minimal Inhibitory concentrations (MICs) for fungi were identified as the low quantity at which there is no visible growth can be seen [34].

Statistical analysis. The mean and standard error were used to express all the data. To determine the relationship between qualitative variables, the Chi-square test will be performed. When more than 25% of the cells have an anticipated count of less than 5, the Fisher exact test will be applied for 2x2 qualitative variables. When comparing the mean and SD of two sets of quantitative normally distributed data, the Student T-test will be employed, whereas the Mann Whitney test will be used when the data is not normally distributed. When comparing three or

Table 1. Primers sequences, target genes, amplicon sizes and cycling conditions.

Target gene	Primers sequences	Amplified segment (bp)	Primary denaturation	Amplification (35 cycles)			Final extension
				Secondary denaturation	Annealing	Extension	
ALS3 [30]	CTGGACCACCAGGAAACACT	122	94°C 5 min.	94°C 30 sec.	60°C 30 sec.	72°C 30 sec.	72°C 7 min.
	ACCTGGAGGAGCAGTCAAAG						
RAS1 [31]	CCCAACTATTGAGGATTCTTATCGTAAA	106	94°C 5 min.	94°C 30 sec.	60°C 30 sec.	72°C 30 sec.	72°C 7 min.
	TCTCATGGCCAGATATTCTTCTTG						
HYR1 [32]	CGTCAACCTGACTGTTACATC	243	94°C 5 min.	94°C 30 sec.	55°C 30 sec.	72°C 30 sec.	72°C 7 min.
	TCTACGGTGGTATGTGGAAC						
SAP4 [33]	GCT CTT GCT ATT GCT TTA TTA	394	94°C 5 min.	94°C 30 sec.	49°C 40 sec.	72°C 40 sec.	72°C 10 min.
	TAG GAA CCG TTA TTC TTA CA						

<https://doi.org/10.1371/journal.pone.0269864.t001>

more groups with quantitative normally distributed data, the one-way analysis of variance (ANOVA) test will be performed, whereas the Kruskal-Wallis test will be used when the data is not normally distributed. When the P-value is less than 0.05, it is considered statistically significant.

Results

UV-vis analysis

The hydrothermal synthesis of T/AgNPs using *Thymus vulgaris* plant extract was detected by visual inspection of the fabricated samples in addition, to monitoring the UV-vis spectra. Alteration of color to yellowish-brown in aqueous solution confirmed the formation of silver nanoparticles [33]. It was observed the color change of colorless solution of silver nitrate to yellowish-brown after 10 min of the addition of extract sample owing to the preparation of silver nanoparticles and this was evaluated by using UV-vis spectrophotometer as depicted in (Fig 2). It was observed that nanoparticles were stable for a long time without being agglomerated. A small band at 438 nm was observed which appeared in the absorption spectra of the fabricated sample (0.1 ml sample). If the concentration of plant extract was increased, the band was positioned from 438 nm to 425 nm.

This band was identified as the absorption by colloidal silver nanoparticles in the visible region (380–450 nm) because of the excitation of surface plasmon vibrations [35]. The intensity of peaks increased and this is an indication of the increase in the concentration of silver nanoparticles [36]. In addition, it was observed that the shifting of the band to a lower wavelength from the maximum absorption wavelength indicated the formation of small-sized Ag nanoparticles with an increased amount of *Thymus vulgaris*. So, it is manifested that there is a

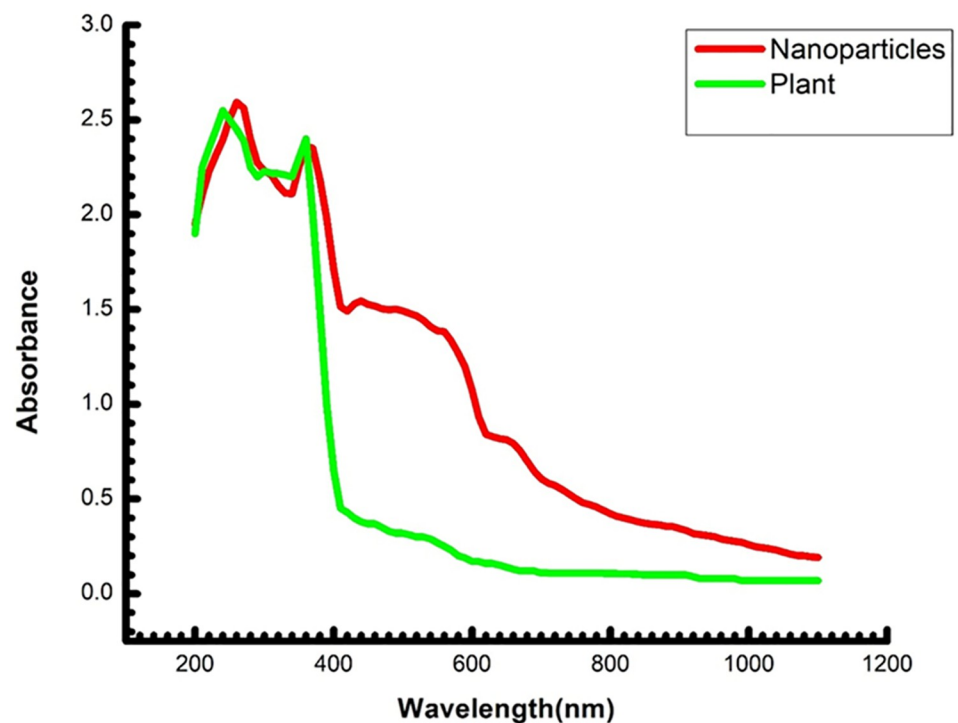


Fig 2. UV-vis spectra of plant extract (green) and silver nanoparticles (red).

<https://doi.org/10.1371/journal.pone.0269864.g002>

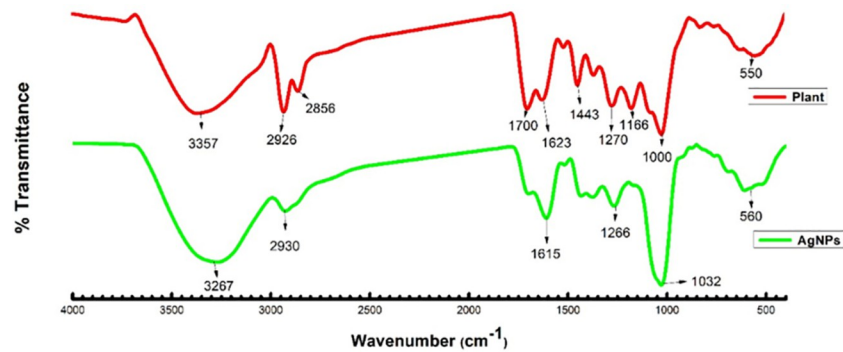


Fig 3. FTIR spectrum of plant extract (red) and silver nanoparticles (green).

<https://doi.org/10.1371/journal.pone.0269864.g003>

successful reduction of silver nanoparticles using *Thymus vulgaris* extract. The stability of silver nanoparticles after various intervals of time was not determined because it is well reported that *Thymus Vulgaris* mediated synthesis yields stable silver nanoparticles [37–40].

Fournier infrared analysis (FTIR)

The identification of biomolecules that are responsible for the reduction and stabilization of silver nanoparticles was detected by FTIR. *Thymus vulgaris* has a heavy amount of protein and is highly concentrated in amino acids [41]. FTIR measurements for *Thymus vulgaris* extract and reduced silver nanoparticles were depicted in (Fig 3). FTIR transmittance peak at 3357 cm^{-1} was detected for *Thymus vulgaris* extract, which was allotted to OH stretching vibration, which become narrow and shifted to the high region at 3267 cm^{-1} . Other bands at 1700 and 1623 cm^{-1} were due to amide I and at 1443 cm^{-1} was assigned to amide II respectively and the peak at 1270 cm^{-1} corresponds to amide III [28, 42–44].

The modification in structure is an indication that the reduction, as well as stabilization of silver nanoparticles, advanced through the coordination between the nitrogen atom of the amide group as well as silver ions. It was shown by FTIR measurements that the amide group of protein has a greater capacity to bind metal. The proteins play a significant role as a capping agent as well as preventing the aggregation of nanoparticles.

High-resolution transmission electron microscopy (HRTEM) analysis

TEM measurements are proceeded to evaluate the particle size as well as size distribution for the fabricated nanoparticles (Fig 4). shows HRTEM images registered from the drop coated HRTEM grid of the manufactured Ag nanoparticles. Nanoparticles with agglomeration and spherical shape were depicted in micrographs which are of course due to the aggregation of silver nanoparticles. It is observed that the less dense region around the black spots (nanoparticles) in the HRTEM image could be attributed to the covering of *Thymus vulgaris* extract.”. At some level of *Thymus vulgaris* extract content, all the nanoparticles are covered, therefore stabilization occurs. So, *Thymus vulgaris* extract is utilized defensive agents to prohibit the aggregation through interaction with initial nanoparticles. and this is in a good agreement explanation of UV–vis spectroscopy results, which is distinguished from well-dispersed silver nanoparticles. The average size of T/AgNPs is determined as 21 nm. The size of each nanoparticle was calculated by using the software in the JEOL-JEM-2100 version and by scale (manually) with reference to the resolution of the image.

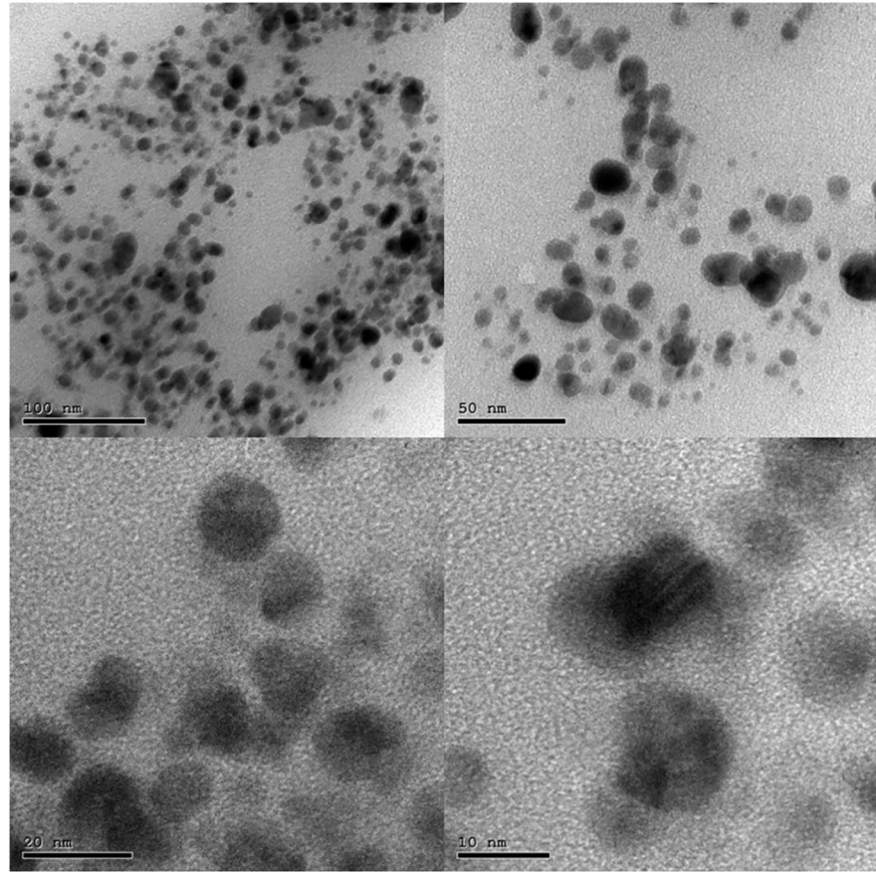


Fig 4. HRTEM image of silver nanoparticles.

<https://doi.org/10.1371/journal.pone.0269864.g004>

Atomic force microscope (AFM) analysis

The atomic force of microscopy was utilized for the determination of morphology and agglomeration of silver nanoparticles using *Thymus vulgaris* extract as shown in (Fig 5). Individual particles, as well as clusters of particles, can also be identified with the AFM. Microscope pictures are crucial in research and development initiatives, as well as when fixing quality control problems. The AFM allows for three-dimensional viewing. The vertical, or Z, axis resolution is restricted by the instrument's vibration environment, whereas the horizontal, or X-Y, axis resolution is limited by the diameter of the scanning tip. Agglomeration of silver nanoparticles biosynthesized on the surface.

Antimicrobial activity

The antifungal treatment was performed by determining the clear inhibition zone supplied with 0.031–0.5mg/mL of silver nanoparticles. Within this range of concentration, the change and visibility of results were prominent. The development of the *Candida* population was observed to decrease by supplying 0.5 mg/mL of T/AgNPs (Fig 6). The greater inhibition zone (22 mm) was monitored for *Candida albicans*, The MICs value observed for T/AgNPs from 0.125–0.250 mg/mL against *Candida* and bacteria species while MBCs and MFCs value obtained was 0.250 and 0.5000 mg/mL respectively. In the present research T/AgNPs with

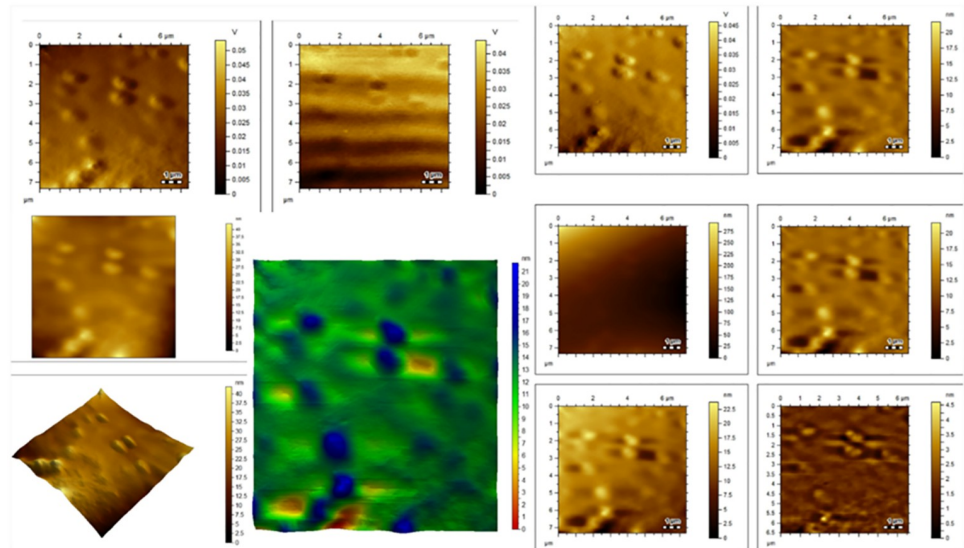


Fig 5. AFM images of *Thyme* based silver nanoparticles (T/AgNPs). “The AFM images display dense aggregates of quasi-spherical AgNPs with an average size of 22 nm. The aggregation shown in AFM images is attributed to the sampling process for AFM leading to dropping a few drops of NPs solution on a silica glass plate and allowing drying to get a thin film of NPs. This will allow the NPs to be clustered together. The AFM images confirm the narrow particle size distribution obtained from TEM images”.

<https://doi.org/10.1371/journal.pone.0269864.g005>

MIC values ranging from 156.25 to 1,250 $\mu\text{g/mL}$ and MFC values ranging from 312.5 to 5,000 $\mu\text{g/mL}$ against *Candida kruzei*, *Candida glabrata* and *Candida albicans*. It was indicated from MIC and MFC values that T/AgNPs had a greater potential for anticandidal activity. Moreover, Different amount of T/AgNPs ranging from 62.5 to 1000 $\mu\text{g/mL}$ was also applied to check the effect on the development of *Candida tropicalis*, *Candida famata* and *Candida albicans* species, followed by decreased growth of *Candida* species at all concentration of the

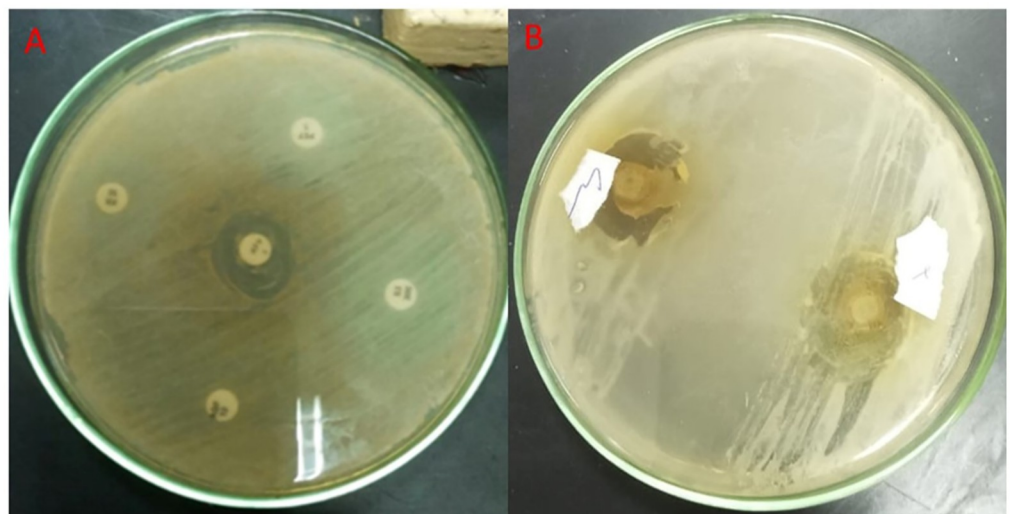


Fig 6. Selected disks show the disk diffusion (antibacterial) activity of silver nanoparticles. (A) Inhibition zone present around the disc dipped in AgNPs and (B) inhibition zone absent around the disc (control).

<https://doi.org/10.1371/journal.pone.0269864.g006>

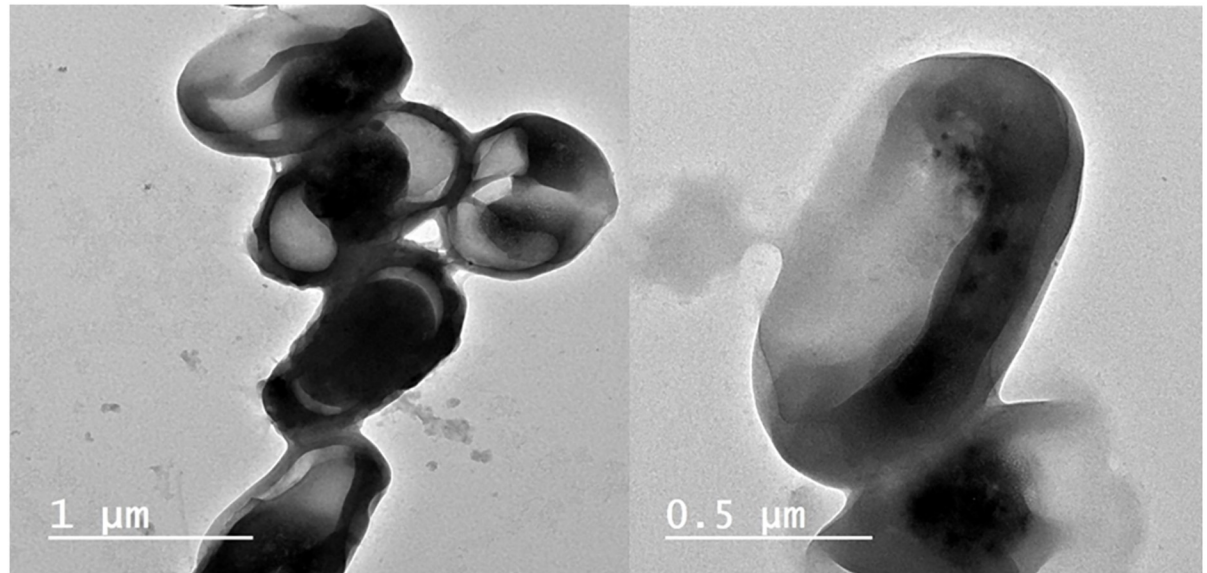


Fig 7. TEM images of the effect of *Thymus vulgaris* silver nanoparticles on *Candida*; destruction of the fungal cell wall with disruption of membrane.

<https://doi.org/10.1371/journal.pone.0269864.g007>

sample. The *Candida* species growth increases rapidly in the dearth of T/AgNPs. However, when the high quantity of T/AgNPs from 500 to 1000 $\mu\text{g}/\text{mL}$ was applied, the *Candida* cells growth was ceased. It has been shown (Fig 6) that the growth inhibition of *Candida* cells was increased with an increased amount of T/AgNPs. The Minimal Inhibitory concentrations (MICs) for fungi were identified as the lowest quantity at which no visual growth was observed. The Minimum fungicidal concentration (MFC) [45, 46] was defined as the lowest drug concentration at which subcultures yielded negative findings or less than three colonies, indicating that >99% of the original inoculum had died.

Morphological and ultrastructural alteration caused by T/AgNPs

The structural and morphological modifications due to T/AgNPs on *Candida albicans* were detected by TEM. It was detected that when *Candida albicans* cells were subjected to 50 and 100 $\mu\text{g}/\text{mL}$ T/AgNPs, a remarkable change in the cell wall and cell membrane was observed (Fig 6). It was found from TEM analysis (Fig 7) that T/AgNPs were adhered not only on the surface of the cell wall and membrane but also penetrate the cell and stored in the cytoplasm followed by the rupturing of the cell wall and destruction of the cytoplasmic membrane (Fig 6). The recent TEM analysis is in good agreement with the previous work on morphological analysis of the effects of T/AgNPs on *Candida albicans* [47]. The exact Anticandidal mechanism of nanostructured material is not known. Kim et al studied that the cell membrane and cell wall of the *Candida albicans* species were destroyed by T/AgNPs due to the formation of “pits and holes” on the surface which prevents the process of budding and results in cell death [48]. It is also reported that the antifungal activity of AgNPs is may be due to inhibition of β -glucan synthase and structural modifications of cell walls which lose their proper functioning and are followed by cell death [49]. Furthermore, in other literature, it was reported that T/AgNPs enhance apoptosis in mitochondria, DNA, and nuclear fragmentation, phosphatidylserine externalization as well as the activation of metacaspases in *Candida albicans* and leads to cell destruction due to the build-up of intercellular ROS. Radhakrishnan et al studied that

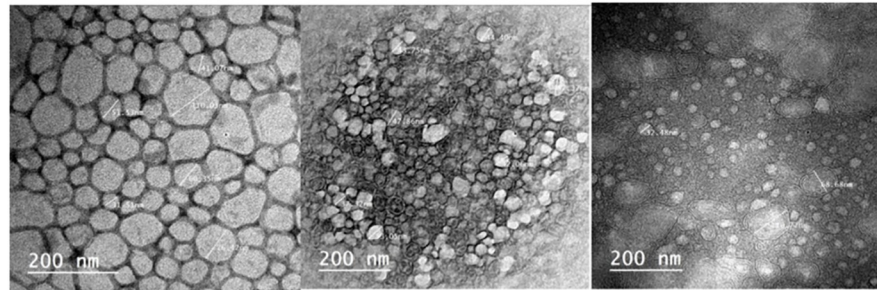


Fig 8. TEM images of SIL (Solid Immersion Lens) showing shrinkage of *Candida albicans* isolates after addition of biologically active silver nitrate particles.

<https://doi.org/10.1371/journal.pone.0269864.g008>

Candida albicans cell destruction is not only due to the accumulation of ROS but also the T/AgNPs affect the cellular microenvironment membrane fluidity, structure, and ultrastructure, cellular ergosterol levels, as well as fatty acid composition, particularly oleic acid, which is essential for hyphal morphogenesis [50].

Candida albicans isolate is resistant to antifungal agents; Nystatin 100 μ g, miconazole (10 μ g), Clotrimazole (50 μ g), Flucytosine (25 μ g) and sensitive to Fluconazole(25 μ g). taking subcultures on the middle plate showing that the *Candida* isolates are resistant to *Thymus vulgaris* alone (lower part) and sensitive to silver nitrate alone; the zone of inhibition increases on the addition of biologically active silver nitrate solution in the sabrouds agar plate on the right.

High-resolution Transmission Electron Microscopy (HRTEM)

To visualize the action of biologically active silver nitrate on *Candida albicans* isolates (Figs 8–11) After growth, the fungal cells were centrifuged as well as fixed with 2.5% glutaraldehyde as well as 4% paraformaldehyde (Sigma-Aldrich) and finally contrasted in the solution of 5%

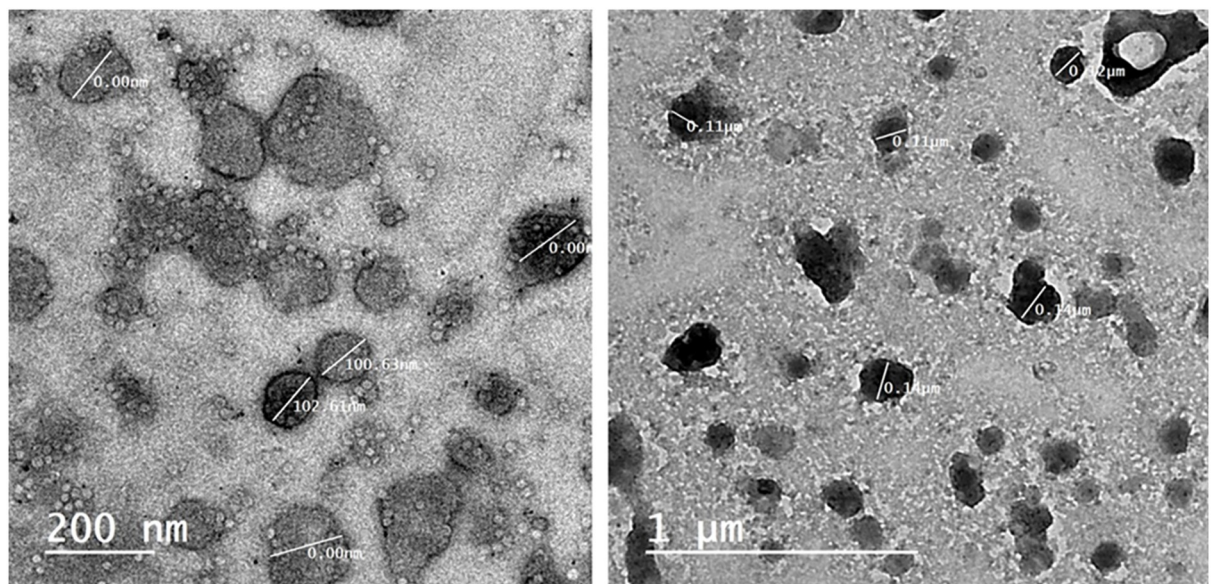


Fig 9. TEM images showing intracellular biologically active T/AgNPs and cellular disruption.

<https://doi.org/10.1371/journal.pone.0269864.g009>

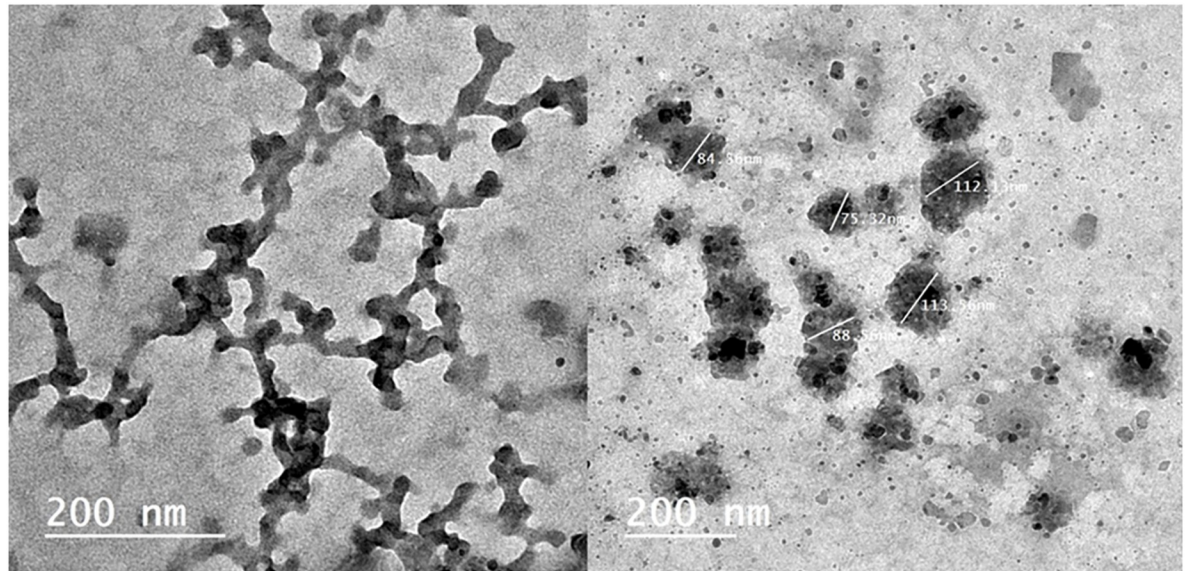


Fig 10. TEM images of the effect of biologically active silver nitrate on *Candida albicans* isolates (image contains disrupted cells).

<https://doi.org/10.1371/journal.pone.0269864.g010>

uranyl acetate. Dehydration was performed using acetone (Sigma-Aldrich). The samples were analyzed under a transmission electron microscope (Thermo Fisher Scientific, USA).

The sociodemographic features, clinical and laboratory data and prognosis of the studied patients with and without fungal growth are mentioned in (Table 2). *Candida albicans* isolates features as mentioned in (Table 3) regarding antifungal sensitivity and virulence factors.

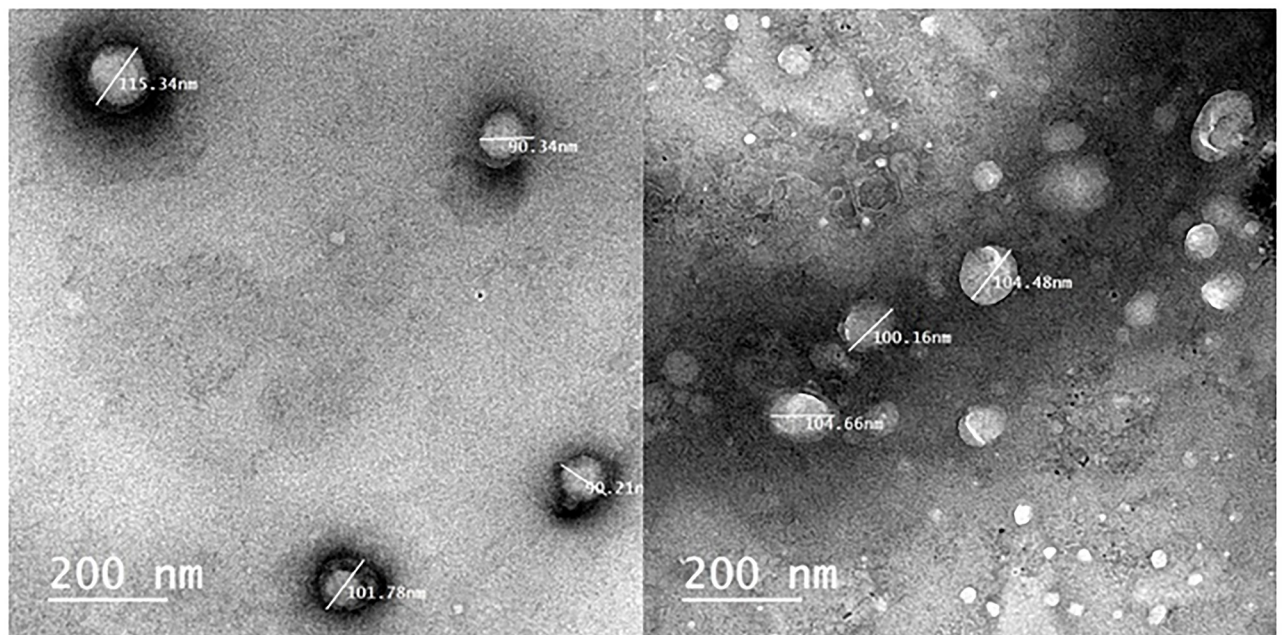


Fig 11. TEM images of intracellular and extracellular distribution of biologically active silver nitrate (measured cells are disrupted).

<https://doi.org/10.1371/journal.pone.0269864.g011>

Table 2. Demographic, clinical-laboratory data, and prognosis of patient groups.

Category		Result		Total	Test	p-value
		Patients without fungal growth N = 14	Patients with fungal growth N = 46			
Sex	Male	9 (64.3%)	32 (69.6%)	41 (68.3%)	$X^2 = 0.138$	0.749
	Female	5 (35.7%)	14 (30.4%)	19 (31.7%)		
Age	Mean \pm Std Deviation	50.93 \pm 6.866	51.96 \pm 7.489	51.72 \pm 7.305	U = 0.315	0.753
	N Median	14 52.00	46 52.00	60 52.00		
	Minimum-Maximum	33–60	24–66	24–66		
Sample	Ascitic	0(0.0%)	1(2.2%)	1(1.7%)	LR = 3.7	0.589
	bedsore	1(7.1%)	2(4.3%)	3(5.0%)		
	Blood	7(50.0%)	16(34.8%)	23(38.3%)		
	cannula site	0(0.0%)	1(2.2%)	1(1.7%)		
	sputum	5(35.7%)	15(32.6%)	20(33.3%)		
Urine	1(7.1%)	11(23.9%)	12(20.0%)			
Nasal SARSCOV2PCR	Negative	0 (0.0%)	1	1	Fisher = 0.31	0.767
	Positive	14(100.0%)	2.2% 45 97.8%	1.7% 59 98.3%		
RBS	Mean \pm	107.29	119.09	116.33	U = 0.861	0.39
	SD	12.755	59.450	52.506		
	N	14	46	60		
	Median	102.00	101.00	102.00		
	(Min-Max)	98 147	82 400	82 400		
CRP	Mean \pm	50.57	53.67	52.91	U = 0.195	0.845
	SD	36.091	41.095	39.633		
	N	14	43	57		
	Median	46.00	48.00	47.00		
	(Min-Max)	12 140	8 225	8 225		
CBC(WBCS)	Mean \pm	7.014	7.941	7.725	U = 2.258	0.024*
	SD	5.7567	4.5884	4.8493		
	N	14	46	60		
	Median	4.150	6.450	6.250		
	(Min-Max)	3.1 19.8	3.1 19.8	3.1 19.8		
Lymphocytes	Mean \pm SD	68.186 \pm 160.9142	21.843 \pm 12.0892	32.657 \pm 78.7876	U = 1.19	0.234
	N Median	14 25.550	46 16.800	60 18.250		
	(Min-Max)	6.0–625.0	6.5–54.3	6.0–625.0		
ESR	Mean \pm SD	47.71 \pm 30.139	45.04 \pm 30.663	45.67 \pm 30.308	U = 0.307	0.759
	N Median	14 51.00	46 40.00	60 40.00		
	(Min-Max)	8–85	5–110	5–110		
serum ferritin	Mean \pm SD	542.93 \pm 231.288	553.07 \pm 291.897	550.70 \pm 277.113	U = 0.105	0.916
	N Median	14 506.00	46 519.00	60 506.00		
	(Min-Max)	320–1150	25–1150	25–1150		
D-Dimer	Mean \pm SD	23.2857 \pm 80.22222	8.6972 \pm 44.2214	12.1012 \pm 54.2977	U = 0.74	0.459
	N Median	14 2.0000	46 2.0000	60 2.0000		
	(Min-Max)	1.00–302.00	.00–302.00	.00–302.00		
LDH	Mean \pm SD	543.64 \pm 186.578	640.04 \pm 262.926	617.55 \pm 249.173	U = 1.006	0.315
	N Median	14 542.50	46 654.00	60 555.00		
	(Min-Max)	204–876	204–1234	204–1234		
Prognosis	Death	0 0.0%	4 8.7%	4 6.7%	Fisher = 1.3	0.564
	Recovery	14 100.0%	42 91.3%	56 93.3%		

<https://doi.org/10.1371/journal.pone.0269864.t002>

Table 3. The sociodemographic, laboratory, antifungal sensitivity, virulence factors in *Candida albicans* versus *Candida non-albicans* isolates.

Category		Candida		Total	Test	p-value
		<i>Candida albicans</i> N = 33	<i>Candida non albican</i> N = 10			
Sex	Male	24	5	29	X ² = 1.8	0.179
	Female	72.7%	50.0%	67.4%		
		9	5	14		
		27.3%	50.0%	32.6%		
Age	Mean	52.12	50.00	51.63	U = 0.403	0.702
	Std. Dev.	5.830	11.776	7.512		
	N	33	10	43		
	Median	51.00	53.50	52.00		
	Minimum	43	24	24		
	Maximum	66	63	66		
Sample	ascitic	1	0	1	LH = 2.7	0.745
	bedsore	3.0%	0.0%	2.3%		
	Blood	2	0	2		
	cannula site	6.1%	0.0%	4.7%		
	sputum	10	4	14		
	Urine	30.3%	40.0%	32.6%		
		1	0	1		
		3.0%	0.0%	2.3%		
		10	4	14		
		30.3%	40.0%	32.6%		
	9	2	11			
	27.3%	20.0%	25.6%			
CORAD	4	31	9	40	Fisher = 0.184	0.558
	5	93.9%	90.0%	93.0%		
		2	1	3		
		6.1%	10.0%	7.0%		
Nasal SARSICOV2PCR	Negative	1	0	1	Fisher = 0.31	1.00
	Positive	32	10	42		
		97.0%	100.0%	97.7%		
RBS	Mean±	118.00	113.60	116.98	U = 0.202	0.840
	SD	62.068	40.716	57.393		
	N	33	10	43		
	Median	100.00	106.00	102.00		
	(Min-Max)	87	82	82		
		400	225	400		
CRP	Mean±	55.69	52.67	55.02	U = 0.315	0.752
	SD	44.397	31.149	41.512		
	N	32	9	41		
	Median	44.00	50.00	48.00		
	(Min-Max)	8	12	8		
		225	125	225		
CBC(WBCS)	Mean±	7.679	9.440	8.088	U = 1.497	0.134
	SD	4.6798	4.7984	4.7103		
	N	33	10	43		
	Median	6.400	6.850	6.500		
	(Min-Max)	3.1	5.4	3.1		
		19.8	18.0	19.8		
Lymphocytes	Mean±	22.339	16.700	21.028	U = 0.792	0.428
	SD	12.8928	6.6663	11.9155		
	N	33	10	43		
	Median	17.200	15.000	16.400		
	(Min-Max)	6.5	7.0	6.5		
		54.3	31.0	54.3		

(Continued)

Table 3. (Continued)

Category		Candida		Total	Test	p-value
		Candida albican N = 33	Candida non albican N = 10			
ESR	Mean±	46.67	44.60	46.19	U = 0.217	0.829
	SD	31.075	29.710	30.425		
	N	33	10	43		
	Median	40.00	35.00	40.00		
	(Min-Max)	5 110	6 100	5 110		
serum ferritin	Mean±	569.61	514.80	556.86	U = 0.374	0.708
	SD	286.640	285.329	283.891		
	N	33	10	43		
	Median	540.00	519.00	540.00		
	(Min-Max)	98 1150	25 1150	25 1150		
D-Dimer	Mean±	11.3052	2.2000	9.1877	U = 0.207	0.836
	SD	52.19852	1.03280	45.73104		
	N	33	10	43		
	Median	2.0000	2.0000	2.0000		
	(Min-Max)	.00 302.00	.00 4.00	.00 302.00		
LDH	Mean±	645.88	703.10	659.19	U = 0.504	0.615
	SD	252.923	292.207	260.066		
	N	33	10	43		
	Median	663.00	732.50	663.00		
	(Min-Max)	204 1234	220 1038	204 1234		
Fluconazole	S	20	3	23	X2 = 2.89	0.089
	R	60.6%	30.0%	53.5%		
		13	7	20		
		39.4%	70.0%	46.5%		
Miconazole	S	19	2	21	X2 = 4.337	0.037*
	R	57.6%	20.0%	48.8%		
		14	8	22		
		42.4%	80.0%	51.2%		
Nystatin	S	23	4	27	X2 = 2.897	0.089
	R	69.7%	40.0%	62.8%		
		10	6	16		
		30.3%	60.0%	37.2%		
Clotrimazole	S	18	3	21	X2 = 1.85	0.174
	R	54.5%	30.0%	48.8%		
		15	7	22		
		45.5%	70.0%	51.2%		
Fluocytosin	S	9	1	10	X2 = 1.28	0.257
	R	27.3%	10.0%	23.3%		
		24	9	33		
		72.7%	90.0%	76.7%		
RAS1	Negative	0	5	5	Fisher = 18.6	0.0001**
	Positive	0.0%	50.0%	11.6%		
		33	5	38		
		100.0%	50.0%	88.4%		
ALS3	Negative	0	4	4	Fisher = 14.55	0.002**
	Positive	0.0%	40.0%	9.3%		
		33	6	39		
		100.0%	60.0%	90.7%		
Hyr1	Negative	3	7	10	X2 = 15.9	0.0001**
	Positive	9.1%	70.0%	23.3%		
		30	3	33		
		90.9%	30.0%	76.7%		

(Continued)

Table 3. (Continued)

Category		Candida		Total	Test	p-value
		Candida albican N = 33	Candida non albican N = 10			
SAP4	Negative	1	4	5	Fisher = 10.2	0.007**
	Positive	32 97.0%	6 60.0%	38 88.4%		
biosynthetic anti-fungal	S	21	5	26	X2 = 0.597	0.44
	R	12 36.4%	5 50.0%	17 39.5%		
Silver nanoparticles plus biosynthetic	S	31	9	40	X2 = 0.573	1.00
	R	2 6.1%	0 0.0%	2 4.8%		
Prognosis	death	0	4	4	Fisher = 14.55	0.002**
	recovery	33 100.0%	6 60.0%	39 90.7%		

<https://doi.org/10.1371/journal.pone.0269864.t003>

Secreted Aspartic Protease gene (SAP4) was detected at 394 bp, RAS1 was detected at 106 bp, Hyphal-Associated Adhesin (HYR1) gene was detected at 243 bp and agglutinin-like sequence gene (ALS3) was detected at 122 bp (Fig 12). Fig 13 show the effect of *Thymus vulgaris* alone and after union with silver nitrate particles on *Candida albicans* isolates in comparison to other antifungal agents.

Candida species, *Aspergillus*, and *P. jirovecii* infections were found in critically unwell COVID-19 patients. parenteral feeding, broad-spectrum anti-bacterial medication, mechanical ventilation, indwelling central venous as well as bladder catheters, lymphopenia, comorbidities, older age, and corticosteroids are all prevalent in COVID-19 patients admitted to the ICU. The goal of this study was to characterise fungal infection in COVID-19 patients while also investigating the antifungal effects of silver nitrate biosynthesized by *Thymus vulgaris*.

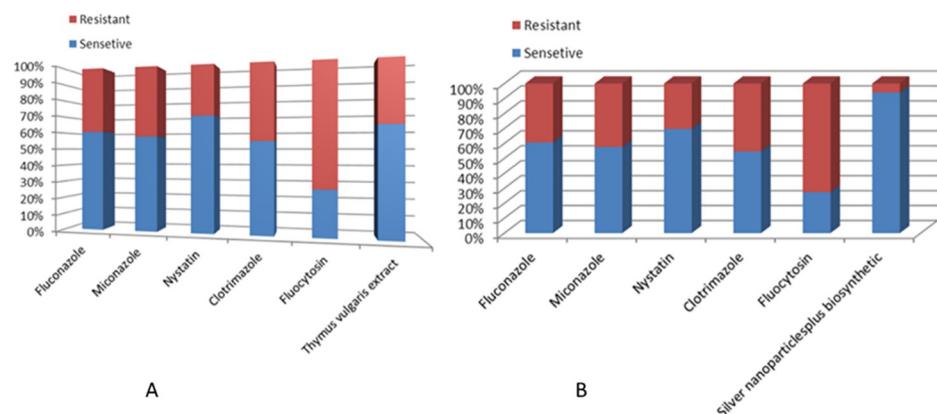


Fig 12. (A) The percentage of resistant isolates to chemical antifungal agents and T/AgNPs. (B) Anti-fungal sensitivity testing of commercial antifungal versus biogenic silver nitrate.

<https://doi.org/10.1371/journal.pone.0269864.g012>

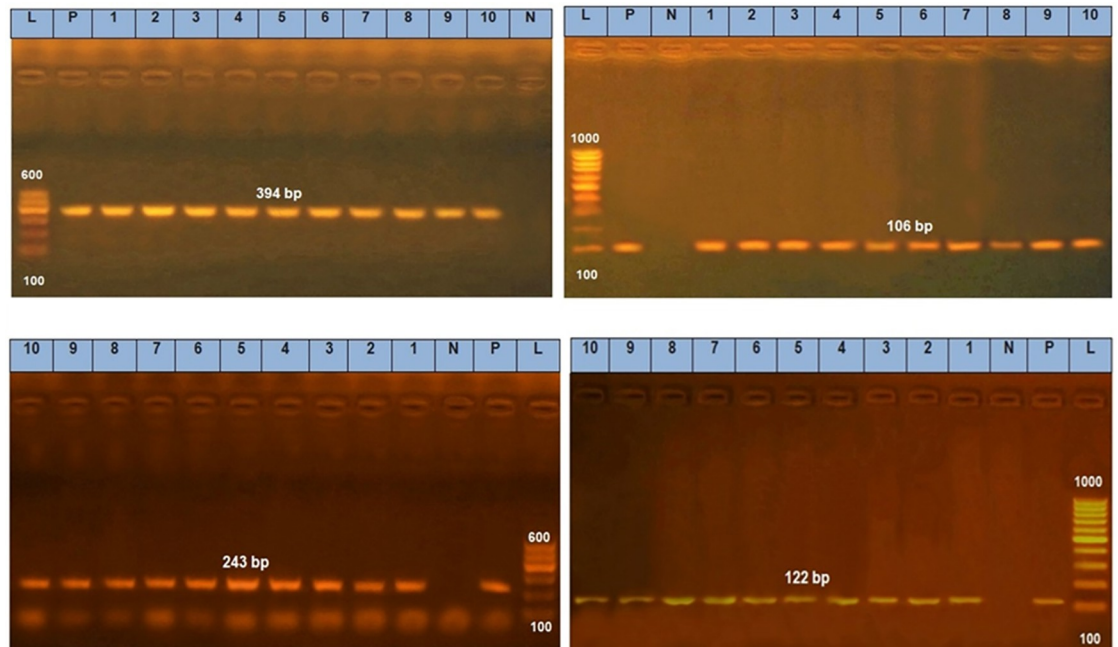


Fig 13. Gel electrophoresis of *Candida* virulence genes, Secreted Aspartic Protease gene (SAP4) was detected at 394 bp, RAS1 was detected at 106 bp, Hyphal-Associated Adhesin (HYR1) gene was detected at 243 bp and agglutinin-like sequence gene (ALS3) was detected at 122 bp.

<https://doi.org/10.1371/journal.pone.0269864.g013>

Discussion

Biogenically synthesized silver nanoparticles have been potent therapeutic agents with prominent antimicrobial properties [51–53]. Although many biogenic nanoparticles have been synthesized still there is need for nanoparticles with precise biological and chemical properties. In this regard use of plant material in the formation of nanoparticles is getting more and more attention [54, 55]. Many scientists used the plant material (bark, leaves, stem, roots, leaves) in the successful synthesis of silver nanoparticles [56–59]. In this study, the hydrothermal method has been adopted for the biogenic synthesis of silver nanoparticles using *Thymus vulgaris* extract. It is the first time use of *Thymus vulagr*is extract in a hydrothermal approach for the synthesis of nanoparticles. The main advantage of this method is that it can produce a bulk amount of silver nanoparticles and the efficiency of this procedure is very much high as compared to other known methods [60–62]. Which may perk from the economical and ecological facet. It is well documented that the use of plant extract in the synthesis of nanoparticles leads to nontoxic properties and natural capping agents [63, 64]. The maximum absorbance of silver nanoparticles has been observed in the UV-visible spectrum at 438 nm to 425 nm due to the surface plasmon vibration in nanoparticles, confirming their synthesis. The results presented here are in good agreement with the previous reports [65–71]. Additionally synthesized T/AgNPs have potential anticandidal properties. FTIR spectrum of T/AgNPs reveals the absorbance peak with variable band intensity as compared to the FTIR spectrum of plant extract [72, 73]. This shifting of absorbance peak may be due to the involvement of biomolecules in the reduction and stabilization of silver ions to silver (0) [74–76]. The HRTEM study indicates that most of the nanoparticles are almost spherical. Very few clusters have been observed that may be size variation or gathering of individual particles. Various sizes of spherical

nanoparticles have been also reported in other studies by TEM analysis [54, 77, 78]. It is well known that the biogenically synthesized AgNPs using plants or microorganisms are an effective way the advancement of secure and proficient control approach against resistant bacteria [79–82]. Herein the potential of synthesized T/AgNPs has been determined in anticandidal activity. In this regard forty-six fungal isolates were obtained from different specimens of 60 COVID-19 inpatients; 33 were *Candida albicans*, 10 *Candida non-albicans* isolates (2 *Candida famata*, 4 *Candida galabrata*, 2 *Candida krusei*, and 2 *Candida tropicalis*). It has been reported that bacteria species and fungi are considered co-infections in critically ill patients with COVID-19, which increases its morbidity and mortality [15]. Numerous strains of *Candida* also have been identified as unique pathogens from COVID-19 patients' pulmonary specimens (TA, BAL as well as BAS) and recognized as a source of co-infections [83] and the frequency of fungal co-infection was significantly greater than previously reported [83].

It is found that *Candida albicans* isolates were highly virulent as 90.7% of isolates had ALS3 and 76.7% had the Hyr1 gene. Hyr1 and Als3 are hypha-specific genes and the hyphal regulator RAS1 is related to adhesion and increase fungal pathogenicity [84]. The RAS1 was prevalent in 88.4%. Ras signalling is crucial to the integration of environmental cues with morphogenesis and virulence [85]. The SAP4 gene was detected in 88.4 percent of *Candida* isolates in this investigation. Twenty secreted aspartic proteinase (Sap) isoenzymes are responsible for *Candida* spp. proteinase's activity. The sap is encoded by ten genes in *Candida*, SAP1–10. Collagen, keratin, and mucus, among other epithelial and mucosal barrier proteins, degrade in the presence of sap [86].

The *Candida* isolates displayed miconazole and clotrimazole resistance in 51.2% of isolates and 100% of aspergillus isolates. Flucytosine resistance occurred in 76.7%, nystatin resistance in 37.2% and fluconazole resistance in 46.5% of isolates. Many researchers have demonstrated that lower *Candida* susceptibility is strongly related to previous antifungal exposures and an unsuitable prior course of antifungal therapy, according to Aldardeer, N. et al, 2020 [87] and Shan, D.N., 2012 mention similar results to other authors [88, 89]. Fluconazole treatment was discovered to be a potential risk for gene mutation and overexposure, which leads to long term fluconazole-resistant *C. parapsilosis* [90]. Plant extracts, which contain biomolecules and plant metabolites including flavonoids, tannins, terpenoids, polyphenols as well as algae and fungal metabolites, have special qualities that allow them to be employed as a reducing and capping agent for the manufacture of pharmaceuticals and stabilisation of nanoparticles (NPs) in a variety of fields, including biomedical, pharmaceutical, and food industries [91]. In the current study, *Thymus vulgaris* derived silver nanoparticles showed a significant antifungal effect with a decrease in the number of resistant isolates than known antifungal fluconazole, miconazole, and nystatin, clotrimazole and flucytosine (P-value <0.05). This finding was in line with Mohammadi, M., et al., who found that Ag NPs manufactured from *thyme* extract have no cytotoxicity at concentrations below 3.5 ppm, making them a viable alternative to Fluconazole for treating superficial fungal infections [38]. Similar results were obtained by Anjugam, M., et al, [92]. The excellent use of plant mediated silver nanoparticles in antibacterial as well as anticancer activities has led to a surge in strong interest among different research groups to employ it, reported by Fahimirad, S., et al, [93].

Conclusion

In our study stable silver nanoparticles were biosynthesized by an eco-benign, one-pot, clean, and useful approach, using leave extract of *Thymus vulgaris*. Hydrothermal synthesis using plant extract is a reliable and safe method. UV-visible spectroscopy, FT-IR, AFM, and TEM techniques were utilized to characterize synthesized T/AgNPs. and confirmed the well-

dispersed nature of nanoparticles. The application of T/AgNPs on virulent strains of *Candida albicans* reveals that they are potent antifungal and anti-virulence agents to fight against *Candida albicans*. The synthesised nanoparticles show good antibacterial activity.

The present research work unlocks numerous ways of advanced studies, such as investigating the inhibition mechanism and destruction of the cell wall of *Candida albicans*. Moreover further In vivo cytotoxicity and biocompatibility studies are needed before being used for biomedical applications.

Acknowledgments

We are thankful to; (1) The Islamia University Bahawalpur 63100, Pakistan for providing basic facilities for the biogenic synthesis of T/AgNPs. (2) Menoufia University, Shebin El-Kom 32511, Egypt for aiding in biological study. (3) Taif University, Taif 21944, Saudi Arabia for assisting informal analysis of T/AgNPs.

Author Contributions

Conceptualization: Muhammad B. Taj.

Formal analysis: Shimaab Abed El-Sattar, Sally W. Elkhadry, Hala El-Refai, Ahmed Salah A. Elgawad.

Methodology: Fatma O. Khalil, Enas M. Ghonaim, Heba Alshater.

Resources: Shimaab Abed El-Sattar, Sally W. Elkhadry, Hala El-Refai, Ahmed Salah A. Elgawad.

Supervision: Muhammad B. Taj.

Writing – original draft: Fatma O. Khalil, Enas M. Ghonaim, Heba Alshater.

Writing – review & editing: Muhammad B. Taj, Omar M. Ali.

References

1. Lai C-C, Shih T-P, Ko W-C, Tang H-J, Hsueh P-R. Severe acute respiratory syndrome coronavirus 2 (SARS-CoV-2) and coronavirus disease-2019 (COVID-19): The epidemic and the challenges. *International journal of antimicrobial agents*. 2020; 55(3):105924. <https://doi.org/10.1016/j.ijantimicag.2020.105924> PMID: 32081636
2. Fani M, Teimoori A, Ghafari S. Comparison of the COVID-2019 (SARS-CoV-2) pathogenesis with SARS-CoV and MERS-CoV infections. *Future Virology*. 2020; 15(5):317–23.
3. Azkur AK, Akdis M, Azkur D, Sokolowska M, van de Veen W, Brügggen MC, et al. Immune response to SARS-CoV-2 and mechanisms of immunopathological changes in COVID-19. *Allergy*. 2020; 75(7):1564–81. <https://doi.org/10.1111/all.14364> PMID: 32396996
4. Gnat S, Łagowski D, Nowakiewicz A, Dyla M. A global view on fungal infections in humans and animals: opportunistic infections and microsporidiosis. *Journal of Applied Microbiology*. 2021; 131(5):2095–113. <https://doi.org/10.1111/jam.15032> PMID: 33556223
5. Ponde NO, Lortal L, Ramage G, Naglik JR, Richardson JP. *Candida albicans* biofilms and polymicrobial interactions. *Critical reviews in microbiology*. 2021; 47(1):91–111. <https://doi.org/10.1080/1040841X.2020.1843400> PMID: 33482069
6. Tängdén T, Giske C. Global dissemination of extensively drug-resistant carbapenemase-producing Enterobacteriaceae: clinical perspectives on detection, treatment and infection control. *Journal of Internal Medicine*. 2015; 277(5):501–12. <https://doi.org/10.1111/joim.12342> PMID: 25556628
7. Gnat S, Łagowski D, Nowakiewicz A. Major challenges and perspectives in the diagnostics and treatment of dermatophyte infections. *Journal of applied microbiology*. 2020; 129(2):212–32. <https://doi.org/10.1111/jam.14611> PMID: 32048417
8. Roco MC. The long view of nanotechnology development: the National Nanotechnology Initiative at 10 years. *Nanotechnology research directions for societal needs in 2020*: Springer; 2011. p. 1–28.

9. Aroob S, Taj MB, Shabbir S, Imran M, Ahmad RH, Habib S, et al. In situ biogenic synthesis of CuO nanoparticles over graphene oxide: A potential nanohybrid for water treatment. *Journal of Environmental Chemical Engineering*. 2021; 9(4):105590.
10. Misra R, Acharya S, Sahoo SK. Cancer nanotechnology: application of nanotechnology in cancer therapy. *Drug discovery today*. 2010; 15(19–20):842–50. <https://doi.org/10.1016/j.drudis.2010.08.006> PMID: 20727417
11. Ahmad F, Taj MB, Ramzan M, Raheel A, Shabbir S, Imran M, et al. Flacourtia indica based biogenic nanoparticles: development, characterization, and bioactivity against wound associated pathogens. *Materials Research Express*. 2020; 7(1):015026.
12. Ahmad F, Taj MB, Ramzan M, Ali H, Ali A, Adeel M, et al. One-pot synthesis and characterization of in-house engineered silver nanoparticles from Flacourtia jangomas fruit extract with effective antibacterial profiles. *Journal of Nanostructure in Chemistry*. 2021; 11(1):131–41.
13. Salleh A, Naomi R, Utami ND, Mohammad AW, Mahmoudi E, Mustafa N, et al. The potential of silver nanoparticles for antiviral and antibacterial applications: a mechanism of action. *Nanomaterials*. 2020; 10(8):1566. <https://doi.org/10.3390/nano10081566> PMID: 32784939
14. Taj MB, Alkahtani MD, Raheel A, Shabbir S, Fatima R, Aroob S, et al. Bioconjugate synthesis, phytochemical analysis, and optical activity of NiFe₂O₄ nanoparticles for the removal of ciprofloxacin and Congo red from water. *Scientific reports*. 2021; 11(1):1–19.
15. Singh A, Gautam PK, Verma A, Singh V, Shivapriya PM, Shivalkar S, et al. Green synthesis of metallic nanoparticles as effective alternatives to treat antibiotics resistant bacterial infections: A review. *Biotechnology Reports*. 2020; 25:e00427. <https://doi.org/10.1016/j.btre.2020.e00427> PMID: 32055457
16. Javed H, Tabassum S, Erum S, Murtaza I, Muhammad A, Amin F, et al. Screening and characterization of selected drugs having antibacterial potential. *Pakistan journal of pharmaceutical sciences*. 2018; 31(3). PMID: 29716876
17. Jafri H, Ahmad I. Thymus vulgaris essential oil and thymol inhibit biofilms and interact synergistically with antifungal drugs against drug resistant strains of *Candida albicans* and *Candida tropicalis*. *Journal de mycologie Medicale*. 2020; 30(1):100911. <https://doi.org/10.1016/j.mycmed.2019.100911> PMID: 32008964
18. Vázquez-Sánchez D, Galvão JA, Ambrosio CM, Gloria EM, Oetterer M. Single and binary applications of essential oils effectively control *Listeria monocytogenes* biofilms. *Industrial Crops and Products*. 2018; 121:452–60.
19. Mehrabyan A, Redfern S. Medicinal plants and their uses and benefits with reference to small farmers in Armenia.
20. El-Sayed SM, El-Sayed HS. Antimicrobial nanoemulsion formulation based on thyme (*Thymus vulgaris*) essential oil for UF labneh preservation. *Journal of Materials Research and Technology*. 2021; 10:1029–41.
21. Aljabeili HS, Barakat H, Abdel-Rahman HA. Chemical composition, antibacterial and antioxidant activities of Thyme essential oil (*Thymus vulgaris*). *Food and Nutrition Sciences*. 2018; 9(05):433.
22. de Oliveira JR, Figueira LW, Sper FL, Meccatti VM, Camargo SEA, de Oliveira LD. Thymus vulgaris L. and thymol assist murine macrophages (RAW 264.7) in the control of in vitro infections by *Staphylococcus aureus*, *Pseudomonas aeruginosa*, and *Candida albicans*. *Immunologic research*. 2017; 65(4):932–43. <https://doi.org/10.1007/s12026-017-8933-z> PMID: 28752199
23. Cavalheiro M, Teixeira MC. *Candida* biofilms: threats, challenges, and promising strategies. *Frontiers in medicine*. 2018; 5:28. <https://doi.org/10.3389/fmed.2018.00028> PMID: 29487851
24. Sardi J, Scorzoni L, Bernardi T, Fusco-Almeida A, Giannini MM. *Candida* species: current epidemiology, pathogenicity, biofilm formation, natural antifungal products and new therapeutic options. *Journal of medical microbiology*. 2013; 62(1):10–24. <https://doi.org/10.1099/jmm.0.045054-0> PMID: 23180477
25. Mishra N, Prasad T, Sharma N, Payasi A, Prasad R, Gupta D, et al. Pathogenicity and drug resistance in *Candida albicans* and other yeast species. *Acta microbiologica et immunologica Hungarica*. 2007; 54(3):201–35.
26. Kong EF, Tsui C, Kucharíková S, Andes D, Van Dijck P, Jabra-Rizk MA. Commensal protection of *Staphylococcus aureus* against antimicrobials by *Candida albicans* biofilm matrix. *MBio*. 2016; 7(5):e01365–16. <https://doi.org/10.1128/mBio.01365-16> PMID: 27729510
27. Taghouti M, Martins-Gomes C, Félix LM, Schäfer J, Santos JA, Bunzel M, et al. Polyphenol composition and biological activity of *Thymus citriodorus* and *Thymus vulgaris*: Comparison with endemic Iberian *Thymus* species. *Food Chemistry*. 2020; 331:127362. <https://doi.org/10.1016/j.foodchem.2020.127362> PMID: 32590268

28. Zayed MF, Eisa WH, Shabaka A. Malva parviflora extract assisted green synthesis of silver nanoparticles. *Spectrochimica Acta Part A: Molecular and Biomolecular Spectroscopy*. 2012; 98:423–8. <https://doi.org/10.1016/j.saa.2012.08.072> PMID: 23010627
29. Ashar A, Bhatti IA, Siddique T, Ibrahim SM, Mirza S, Bhutta ZA, et al. Integrated hydrothermal assisted green synthesis of ZnO nano discs and their water purification efficiency together with antimicrobial activity. *Journal of Materials Research and Technology*. 2021; 15:6901–17.
30. Tsang PW-K, Bandara H, Fong W-P. Purpurin suppresses *Candida albicans* biofilm formation and hyphal development. *PLoS One*. 2012; 7(11):e50866. <https://doi.org/10.1371/journal.pone.0050866> PMID: 23226409
31. Luo G, Ibrahim AS, Spellberg B, Nobile CJ, Mitchell AP, Fu Y. *Candida albicans* Hyr1p confers resistance to neutrophil killing and is a potential vaccine target. *The Journal of infectious diseases*. 2010; 201(11):1718–28. <https://doi.org/10.1086/652407> PMID: 20415594
32. Sikora M, Dabkowska M, Swoboda-Kopec E, Jarzynka S, Netsvyetayeva I, Jaworska-Zaremba M, et al. Differences in proteolytic activity and gene profiles of fungal strains isolated from the total parenteral nutrition patients. *Folia microbiologica*. 2011; 56(2):143–8. <https://doi.org/10.1007/s12223-011-0023-3> PMID: 21455781
33. Song JY, Kim BS. Rapid biological synthesis of silver nanoparticles using plant leaf extracts. *Bioprocess and biosystems engineering*. 2009; 32(1):79–84. <https://doi.org/10.1007/s00449-008-0224-6> PMID: 18438688
34. Silva S, Pires P, Monteiro DR, Negri M, Gorup LF, Camargo ER, et al. The effect of silver nanoparticles and nystatin on mixed biofilms of *Candida glabrata* and *Candida albicans* on acrylic. *Medical mycology*. 2013; 51(2):178–84. <https://doi.org/10.3109/13693786.2012.700492> PMID: 22803822
35. Njagi EC, Huang H, Stafford L, Genuino H, Galindo HM, Collins JB, et al. Biosynthesis of iron and silver nanoparticles at room temperature using aqueous sorghum bran extracts. *Langmuir*. 2011; 27(1):264–71. <https://doi.org/10.1021/la103190n> PMID: 21133391
36. Zhang W, Qiao X, Chen J. Synthesis and characterization of silver nanoparticles in AOT microemulsion system. *Chemical physics*. 2006; 330(3):495–500.
37. Balciunaitiene A, Viskelis P, Viskelis J, Streimikyte P, Liaudanskas M, Bartkiene E, et al. Green synthesis of silver nanoparticles using extract of *Artemisia absinthium* L., *Humulus lupulus* L. and *Thymus vulgaris* L., physico-chemical characterization, antimicrobial and antioxidant activity. *Processes*. 2021; 9(8):1304.
38. Mohammadi M, Shahisaraee SA, Tavajjohi A, Pournoori N, Muhammadnejad S, Mohammadi SR, et al. Green synthesis of silver nanoparticles using *Zingiber officinale* and *Thymus vulgaris* extracts: characterisation, cell cytotoxicity, and its antifungal activity against *Candida albicans* in comparison to fluconazole. *IET nanobiotechnology*. 2019; 13(2):114–9. <https://doi.org/10.1049/iet-nbt.2018.5146> PMID: 31051440
39. De Melo APZ, Maciel MVdOB, Sganzerla WG, da Rosa Almeida A, de Armas RD, Machado MH, et al. Antibacterial activity, morphology, and physicochemical stability of biosynthesized silver nanoparticles using thyme (*Thymus vulgaris*) essential oil. *Materials Research Express*. 2020; 7(1):015087.
40. Azadi M, Moghaddam SS, Rahimi A, Pourakbar L, Popović-Djordjević J. Biosynthesized silver nanoparticles ameliorate yield, leaf photosynthetic pigments, and essential oil composition of garden thyme (*Thymus vulgaris* L.) exposed to UV-B stress. *Journal of Environmental Chemical Engineering*. 2021; 9(5):105919.
41. Wang X, Bunkers GJ. Potent heterologous antifungal proteins from cheeseweed (*Malva parviflora*). *Biochemical and biophysical research communications*. 2000; 279(2):669–73. <https://doi.org/10.1006/bbrc.2000.3997> PMID: 11118343
42. He S, Zhang Y, Guo Z, Gu N. Biological synthesis of gold nanowires using extract of *Rhodospseudomonas capsulata*. *Biotechnology Progress*. 2008; 24(2):476–80. <https://doi.org/10.1021/bp0703174> PMID: 18293997
43. Basavaraja S, Balaji S, Lagashetty A, Rajasab A, Venkataraman A. Extracellular biosynthesis of silver nanoparticles using the fungus *Fusarium semitectum*. *Materials Research Bulletin*. 2008; 43(5):1164–70.
44. Ji Y, Yang X, Ji Z, Zhu L, Ma N, Chen D, et al. DFT-calculated IR spectrum amide I, II, and III band contributions of N-methylacetamide fine components. *ACS omega*. 2020; 5(15):8572–8. <https://doi.org/10.1021/acsomega.9b04421> PMID: 32337419
45. Brilhante RS, Paiva MA, Sampaio CM, Teixeira CE, Castelo-Branco DS, Leite JJ, et al. Yeasts from *Macrobrachium amazonicum*: a focus on antifungal susceptibility and virulence factors of *Candida* spp. *FEMS microbiology ecology*. 2011; 76(2):268–77. <https://doi.org/10.1111/j.1574-6941.2011.01050.x> PMID: 21241340

46. Ciurea CN, Kosovski I-B, Mare AD, Toma F, Pinteau-Simon IA, Man A. Candida and Candidiasis—Opportunism Versus Pathogenicity: A Review of the Virulence Traits. *Microorganisms*. 2020; 8(6):857. <https://doi.org/10.3390/microorganisms8060857> PMID: 32517179
47. Jalal M, Ansari MA, Alzohairy MA, Ali SG, Khan HM, Almatroudi A, et al. Anticandidal activity of bio-synthesized silver nanoparticles: effect on growth, cell morphology, and key virulence attributes of *Candida* species. *International journal of nanomedicine*. 2019; 14:4667. <https://doi.org/10.2147/IJN.S210449> PMID: 31308652
48. Kim K-J, Sung WS, Suh BK, Moon S-K, Choi J-S, Kim JG, et al. Antifungal activity and mode of action of silver nano-particles on *Candida albicans*. *Biometals*. 2009; 22(2):235–42. <https://doi.org/10.1007/s10534-008-9159-2> PMID: 18769871
49. Padhi S, Behera A. Silver-based nanostructures as antifungal agents: Mechanisms and applications. *Silver Nanomaterials for Agri-Food Applications*: Elsevier; 2021. p. 17–38.
50. Radhakrishnan VS, Mudiam MKR, Kumar M, Dwivedi SP, Singh SP, Prasad T. Silver nanoparticles induced alterations in multiple cellular targets, which are critical for drug susceptibilities and pathogenicity in fungal pathogen (*Candida albicans*). *International journal of nanomedicine*. 2018; 13:2647. <https://doi.org/10.2147/IJN.S150648> PMID: 29760548
51. Vickers NJ. Animal communication: when i'm calling you, will you answer too? *Current biology*. 2017; 27(14):R713–R5. <https://doi.org/10.1016/j.cub.2017.05.064> PMID: 28743020
52. Alster CJ, Baas P, Wallenstein MD, Johnson NG, Von Fischer JC. Temperature sensitivity as a microbial trait using parameters from macromolecular rate theory. *Frontiers in microbiology*. 2016; 7:1821. <https://doi.org/10.3389/fmicb.2016.01821> PMID: 27909429
53. Zhang X-F, Liu Z-G, Shen W, Gurunathan S. Silver nanoparticles: synthesis, characterization, properties, applications, and therapeutic approaches. *International journal of molecular sciences*. 2016; 17(9):1534.
54. Nakazato G, Oves M, Prasad R, Qiu W, Li B, Md. Mahidul Islam Masum^{1, 2}, et al. *Nanotechnology for Antimicrobials*. 2020.
55. Krithiga N, Jayachitra A, Rajalakshmi A. Synthesis, characterization and analysis of the effect of copper oxide nanoparticles in biological systems. *Indian journal of nanoscience*. 2013; 1(1):6–15.
56. Al-Otibi F, Perveen K, Al-Saif NA, Alharbi RI, Bokhari NA, Albasher G, et al. Biosynthesis of silver nanoparticles using *Malva parviflora* and their antifungal activity. *Saudi Journal of Biological Sciences*. 2021; 28(4):2229–35. <https://doi.org/10.1016/j.sjbs.2021.01.012> PMID: 33935565
57. Alabdallah NM, Hasan MM. Plant-based green synthesis of silver nanoparticles and its effective role in abiotic stress tolerance in crop plants. *Saudi Journal of Biological Sciences*. 2021; 28(10):5631–9. <https://doi.org/10.1016/j.sjbs.2021.05.081> PMID: 34588874
58. Lediga M, Malatjie T, Olivier D, Ndinteh D, Van Vuuren S. Biosynthesis and characterisation of antimicrobial silver nanoparticles from a selection of fever-reducing medicinal plants of South Africa. *South African Journal of Botany*. 2018; 119:172–80.
59. Roy P, Das B, Mohanty A, Mohapatra S. Green synthesis of silver nanoparticles using *Azadirachta indica* leaf extract and its antimicrobial study. *Applied Nanoscience*. 2017; 7(8):843–50.
60. Nouri A, Yarak MT, Lajevardi A, Rezaei Z, Ghorbanpour M, Tanzifi M. Ultrasonic-assisted green synthesis of silver nanoparticles using *Mentha aquatica* leaf extract for enhanced antibacterial properties and catalytic activity. *Colloid and Interface Science Communications*. 2020; 35:100252.
61. Tippayawat P, Phromviyo N, Boueroy P, Chompoosor A. Green synthesis of silver nanoparticles in aloe vera plant extract prepared by a hydrothermal method and their synergistic antibacterial activity. *PeerJ*. 2016; 4:e2589. <https://doi.org/10.7717/peerj.2589> PMID: 27781173
62. Ocsoy I, Demirbas A, McLamore ES, Altinsoy B, Ildiz N, Baldemir A. Green synthesis with incorporated hydrothermal approaches for silver nanoparticles formation and enhanced antimicrobial activity against bacterial and fungal pathogens. *Journal of Molecular Liquids*. 2017; 238:263–9.
63. Basnet P, Chatterjee S. Structure-directing property and growth mechanism induced by capping agents in nanostructured ZnO during hydrothermal synthesis—A systematic review. *Nano-Structures & Nano-Objects*. 2020; 22:100426.
64. Bose D, Chatterjee S. Biogenic synthesis of silver nanoparticles using guava (*Psidium guajava*) leaf extract and its antibacterial activity against *Pseudomonas aeruginosa*. *Applied Nanoscience*. 2016; 6(6):895–901.
65. Ahmed S, Saifullah, Ahmad M, Swami BL, Ikram S. Green synthesis of silver nanoparticles using *Azadirachta indica* aqueous leaf extract. *Journal of radiation research and applied sciences*. 2016; 9(1):1–7.

66. Thatikayala D, Jayarambabu N, Banothu V, Ballipalli CB, Park J, Rao KV. Biogenic synthesis of silver nanoparticles mediated by *Theobroma cacao* extract: enhanced antibacterial and photocatalytic activities. *Journal of Materials Science: Materials in Electronics*. 2019; 30(18):17303–13.
67. Konappa N, Udayashankar AC, Dhamodaran N, Krishnamurthy S, Jagannath S, Uzma F, et al. Ameliorated antibacterial and antioxidant properties by *Trichoderma harzianum* mediated green synthesis of silver nanoparticles. *Biomolecules*. 2021; 11(4):535. <https://doi.org/10.3390/biom11040535> PMID: 33916555
68. Swilam N, Nemattallah KA. Polyphenols profile of pomegranate leaves and their role in green synthesis of silver nanoparticles. *Scientific Reports*. 2020; 10(1):1–11.
69. Banjare MK, Behera K, Banjare RK, Sahu R, Sharma S, Pandey S, et al. Interaction of ionic liquid with silver nanoparticles: potential application in induced structural changes of globular proteins. *ACS Sustainable Chemistry & Engineering*. 2019; 7(13):11088–100.
70. Meena, Sharma A. Investigation of structural, optical and sensing performance of starch films reinforced with Ag nanoparticles. *International Journal of Polymer Analysis and Characterization*. 2021; 26(5):396–410.
71. Jalilian F, Chahardoli A, Sadrjavadi K, Fattahi A, Shokoohinia Y. Green synthesized silver nanoparticle from *Allium ampeloprasum* aqueous extract: Characterization, antioxidant activities, antibacterial and cytotoxicity effects. *Advanced Powder Technology*. 2020; 31(3):1323–32.
72. Oves M, Aslam M, Rauf MA, Qayyum S, Qari HA, Khan MS, et al. Antimicrobial and anticancer activities of silver nanoparticles synthesized from the root hair extract of *Phoenix dactylifera*. *Materials Science and Engineering: C*. 2018; 89:429–43. <https://doi.org/10.1016/j.msec.2018.03.035> PMID: 29752116
73. Zhang Y-F, Wang X, Kaushik AC, Chu Y, Shan X, Zhao M-Z, et al. SPVec: a Word2vec-inspired feature representation method for drug-target interaction prediction. *Frontiers in chemistry*. 2020; 7:895. <https://doi.org/10.3389/fchem.2019.00895> PMID: 31998687
74. Anandalakshmi K, Venugobal J, Ramasamy V. Characterization of silver nanoparticles by green synthesis method using *Petalium murex* leaf extract and their antibacterial activity. *Applied nanoscience*. 2016; 6(3):399–408.
75. Rezazadeh NH, Buazar F, Matroodi S. Synergistic effects of combinatorial chitosan and polyphenol biomolecules on enhanced antibacterial activity of biofunctionalized silver nanoparticles. *Scientific reports*. 2020; 10(1):1–13.
76. Jain S, Mehata MS. Medicinal plant leaf extract and pure flavonoid mediated green synthesis of silver nanoparticles and their enhanced antibacterial property. *Scientific reports*. 2017; 7(1):1–13.
77. Alsharif SM, Salem SS, Abdel-Rahman MA, Fouda A, Eid AM, Hassan SE-D, et al. Multifunctional properties of spherical silver nanoparticles fabricated by different microbial taxa. *Heliyon*. 2020; 6(5):e03943. <https://doi.org/10.1016/j.heliyon.2020.e03943> PMID: 32518846
78. Acharya D, Singha KM, Pandey P, Mohanta B, Rajkumari J, Singha LP. Shape dependent physical mutilation and lethal effects of silver nanoparticles on bacteria. *Scientific reports*. 2018; 8(1):1–11.
79. Rana KL, Kour D, Yadav N, Yadav AN. Endophytic microbes in nanotechnology: current development, and potential biotechnology applications. *Microbial endophytes*: Elsevier; 2020. p. 231–62.
80. Paul A, Roychoudhury A. Go green to protect plants: repurposing the antimicrobial activity of biosynthesized silver nanoparticles to combat phytopathogens. *Nanotechnology for Environmental Engineering*. 2021; 6(1):1–22.
81. Fatima F, Siddiqui S, Khan WA. Nanoparticles as novel emerging therapeutic antibacterial agents in the antibiotics resistant era. *Biological Trace Element Research*. 2021; 199(7):2552–64. <https://doi.org/10.1007/s12011-020-02394-3> PMID: 33030657
82. Bhattacharya J, Nitnavare R, Shankhpal A, Ghosh S. Microbially synthesized nanoparticles: aspect in plant disease management. *Biocontrol Mechanisms of Endophytic Microorganisms*: Elsevier; 2022. p. 303–25.
83. Pemán J, Ruiz-Gaitán A, García-Vidal C, Salavert M, Ramírez P, Puchades F, et al. Fungal co-infection in COVID-19 patients: Should we be concerned? *Revista iberoamericana de micología*. 2020; 37(2):41–6. <https://doi.org/10.1016/j.riam.2020.07.001> PMID: 33041191
84. Fan Y, He H, Dong Y, Pan H. Hyphae-specific genes HGC1, ALS3, HWP1, and ECE1 and relevant signaling pathways in *Candida albicans*. *Mycopathologia*. 2013; 176(5–6):329–35. <https://doi.org/10.1007/s11046-013-9684-6> PMID: 24002103.
85. Pentland DR, Piper-Brown E, Muhlschlegel FA, Gourlay CW. Ras signalling in pathogenic yeasts. *Microb Cell*. 2017; 5(2):63–73. <https://doi.org/10.15698/mic2018.02.612> PMID: 29417055.
86. Deorukhkar SC, Saini S, Mathew S. Virulence Factors Contributing to Pathogenicity of *Candida tropicalis* and Its Antifungal Susceptibility Profile. *Int J Microbiol*. 2014; 2014:456878. <https://doi.org/10.1155/2014/456878> PMID: 24803934.

87. Aldardeer NF, Albar H, Al-Attas M, Eldali A, Qutub M, Hassanien A, et al. Antifungal resistance in patients with Candidaemia: a retrospective cohort study. *BMC Infect Dis.* 2020; 20(1):55. <https://doi.org/10.1186/s12879-019-4710-z> PMID: 31952505.
88. Shah DN, Yau R, Lasco TM, Weston J, Salazar M, Palmer HR, et al. Impact of prior inappropriate fluconazole dosing on isolation of fluconazole-nonsusceptible *Candida* species in hospitalized patients with candidemia. *Antimicrob Agents Chemother.* 2012; 56(6):3239–43. <https://doi.org/10.1128/AAC.00019-12> PMID: 22411611.
89. Garnacho-Montero J, Diaz-Martin A, Garcia-Cabrera E, Ruiz Perez de Pipaon M, Hernandez-Caballero C, Aznar-Martin J, et al. Risk factors for fluconazole-resistant candidemia. *Antimicrob Agents Chemother.* 2010; 54(8):3149–54. <https://doi.org/10.1128/AAC.00479-10> PMID: 20498325.
90. Souza AC, Fuchs BB, Pinhati HM, Siqueira RA, Hagen F, Meis JF, et al. *Candida parapsilosis* Resistance to Fluconazole: Molecular Mechanisms and In Vivo Impact in Infected *Galleria mellonella* Larvae. *Antimicrob Agents Chemother.* 2015; 59(10):6581–7. <https://doi.org/10.1128/AAC.01177-15> PMID: 26259795.
91. Kshtriya Vivekshinh, Koshti Bharti, Gour N. Green synthesized nanoparticles: Classification, synthesis, characterization, and applications, *Comprehensive Analytical Chemistry*. Comprehensive Analytical Chemistry, Elsevier. 2021. <https://doi.org/10.1016/bs.coac.2020.12.009> (<https://www.sciencedirect.com/science/article/pii/S0166526X20301161>).
92. Anjugam M, Vaseeharan B, Iswarya A, Divya M, Prabhu NM, Sankaranarayanan K. Biological synthesis of silver nanoparticles using beta-1, 3 glucan binding protein and their antibacterial, antibiofilm and cytotoxic potential. *Microb Pathog.* 2018; 115:31–40. <https://doi.org/10.1016/j.micpath.2017.12.003> PMID: 29208541.
93. Fahimirad S, Ajallouei F, Ghorbanpour M. Synthesis and therapeutic potential of silver nanomaterials derived from plant extracts. *Ecotoxicol Environ Saf.* 2019; 168:260–78. <https://doi.org/10.1016/j.ecoenv.2018.10.017> PMID: 30388544.